Ultrasonic welding of 100% lignocellulosic papers

Arnaud Regazzi, Jérémie Viguié, Barthelemy Harthong, Pierre J. J. Dumont, Didier Imbault, Robert Peyroux, Martine Rueff, Quentin Charlier, David Guérin, Laurence Leroy, et al.

Ultrasonic welding of 100% lignocellulosic papers

Arnaud Regazzi[1,2], Jérémie Viguié[4,*], Barthélémy Harthong[1], Pierre J. J. Dumont[3], Didier Imbault[1], Robert Peyroux[1], Martine Rueff[2], Quentin Charlier[1], David Guérin[4], Laurence Leroy[4], Mohammed Krouit[4], and Michel Petit-Conil[4]

[1] *Université Grenoble Alpes, Grenoble INP, CNRS UMR 5518, LGP2, 38000 Grenoble, France*
[2] *Université Grenoble Alpes, Grenoble INP, CNRS, 3SR UMR 5521, 38000 Grenoble, France*
[3] *Université Lyon, INSA Lyon, CNRS UMR 5259, LaMCoS, F-69621 Lyon, France*
[4] *Centre Technique du Papier (CTP), 38044 Grenoble, France*

ABSTRACT

Paper-based packaging materials are generally assembled using adhesives formulated with oil-based polymers. These adhesives make the recyclability of the materials more complex and may be the source of material contamination by mineral oil. In view of developing an adhesive-free process, the potential of ultrasonic compression was investigated in this study. 100% lignocellulosic papers were assembled using an ultrasonic welder dedicated to thermoplastic polymers. For papers containing lignin, the measured peeling strengths were equivalent to those achieved by hot-melt gluing, provided that the water content of papers was well adjusted. At the interface between bonded papers, the fiber network was dense and rather continuous. SEM examinations, 3D X-ray microtomography images, and temperature measurements suggested that the development of adhesion originated to a large extent from a thermoplastic welding mechanism: wood fiber polymers passed their glass transition temperatures, creeped and formed a matrix that coated fibers. Thus, ultrasonic welding appears as an efficient adhesive-free technique for assembling papers that are used in a broad range of packaging applications.

Introduction

In Europe, 50% of paper-based materials are dedicated to packaging and their recyclability rate is 72% [1]. However, packaging materials are generally assembled using adhesives formulated with oil-based polymers such as poly(vinyl acetate) (PVAc), polyethylene (PE) or ethylene vinyl acetate (EVAc). These glues are either hot-melt adhesives, or formulated with a solvent or water, causing potential contamination by mineral oil. They also make the recyclability of the materials more complex because they require a significantly higher energy and create additional waste. Heat-fusible coatings used to seal flexible packaging materials or cellulose-based hygiene products create similar issues, as they are usually based either on PE or on polyacrylate. Therefore, a process capable of assembling papers, paperboards or

Address correspondence to E-mail: Jeremie.Viguie@webCTP.com

https://doi.org/10.1007/s10853-019-03763-7

other cellulose-based packaging materials without any additives would be of great interest.

In the industry of polymers, a variety of welding technologies exists. Among them, ultrasonic welding is a mature technology and widely used for welding thermoplastic polymer parts, assembling nonwovens or sealing packaging. The order of magnitude of the welding time is one second, which makes this process economically attractive and energy efficient. The method consists in converting a high-frequency electrical signal into mechanical vibrations (15–70 kHz) capable of generating localized heating at the interface between two parts in contact. The heating process is initially started by interfacial friction. Once the glass transition temperature of the material is reached, viscoelastic heating becomes predominant [2, 3]. Viscoelastic dissipation provides most of the heat required for welding [4, 5]. The thermoplastic material flows to form a continuous media at the interface after cooling. Wave propagation through the materials might also induce localized heating in the bulk material far from the interface to be welded [6]. However, in the case of paper welding, the small thickness of the layers to be welded (approximately 100 μm) prevents from this potential issue. The remaining question is whether it is possible or not to achieve permanent bonding between paper pulp fibers through localized heating.

Several studies reported the ability of lignocellulose from wood or annual plants to be assembled/bonded without adhesive by static methods like thermo-compression, possibly assisted by injection of steam [7, 8] or by dynamic processes like vibrational welding at low frequency [9–14] or ultrasonic compression [15].

- In thermo-compression, adhesion phenomena are activated at temperatures around 180–200 °C and pressures that range from 5 to 30 MPa. The loading time is several minutes.
- In dynamic processes, the increase in temperature is generated mechanically, by friction and/or viscous dissipation. The temperatures measured by thermocouples [16] or by infrared thermography [10] can reach 250–440 °C. The loading time is a few seconds.

The physicochemical phenomena associated with the development of adhesion have been the subject of significant research efforts in recent years, both on the thermo-compression process [7, 8], and on the friction process [9, 12, 16–18]. Although processes differ in type and loading times, several types of mechanisms contribute to the development of bonding:

- A 'thermoplastic' mechanism: beyond their glass transition temperature (T_g), amorphous polymers of wood, such as hemicelluloses, lignin and amorphous cellulose, tend to creep under the effect of pressure, fill voids within and between fibers and form a matrix embedding the fibers. This phenomenon is considered as the main mechanism responsible for the adhesion during the friction welding of wood [9]. The T_g of wood polymers are dependent on the amount of water originally contained in the fibers. In the dry state, the T_g of the hemicelluloses, lignin and amorphous cellulose is about 170 °C, 200 °C and 220 °C, respectively [19]. At 12% of water, the T_g of the lignin drops to 80 °C. Thus, this mechanism would be activated at 100–120 °C during friction welding or thermo-compression coupled to a steam injection of wood.
- A 'thermosetting' mechanism, which is activated after the 'thermoplastic mechanism' once intimate contact between surfaces is achieved, and involves chemical reactions related to the degradation of the polymers and creation of new compounds. Chemical reactions become significant at high temperature (around 200 °C). FT-IR, 13C CP MAS NMR and XPS analyses were conducted as part of several studies on friction welding or thermo-compression with pre-treatment or steam injection [8, 11, 17]. Coupled with temperature measurements, these studies allowed identifying the chemical reactions involved in the development of adhesion:
  - When the water warms up, it causes a decrease in pH at the interface and promotes protonation of the environment: hydrolysis reactions of polysaccharides occur.
  - Above 140 °C, the condensation reactions of the monomers derived from the hydrolysis take place. The condensation reactions cause the formation of water molecules that are re-employed in the hydrolysis process.

- Lignin also undergoes a high-temperature hydrolysis (close to 200 °C). The molecules thus obtained can be condensed with the elements in solution or condense themselves. The novel lignin–sugars complexes mechanically reinforce the matrix and, from this point of view, improve adhesion. However, the material becomes more brittle with the appearance of micro-cracks and voids at the composite interface.

- A 'reinforcement' mechanism: measurements established that the degree of crystallinity increases in the bonded zones [17], not only due to the hydrolysis of amorphous polymers but also to a potential co-crystallization of the cellulose microfibrils [7]. The new crystals may act as reinforcements of the lignin matrix sugars [8].

Within this context, the objective of this study was to determine the potential of assembling papers by ultrasonic welding. The performance of a paper-to-paper welded joint was assessed. The influence of the nature of the pulp and the moisture content of paper were investigated. The evolution of the temperature at the welded joint was measured, and the structural properties of the joints were characterized. Finally, results were discussed to give insights on the mechanisms responsible for the development of adhesion.

Materials and methods

Materials

Pulp

To study the influence of the chemical composition of paper, four different softwood pulps were used:

- Thermo-mechanical pulp (TMP)—Fibers were extracted from wood by processing wood chips using heat and a mechanical refining movement. This process tends to preserve the native plant material, where lignin represents more than 25% of the fiber composition.
- Chemi-thermo-mechanical pulp (CTMP)—In this case, wood chips were pre-treated with chemicals (sodium hydroxide, sodium sulfite or others) prior to refining with equipment or devices similar than those used for TMP. Compared to TMP, extractives are removed and the lignin content is slightly decreased.
- Unbleached kraft pulp (UKP)—This process consists in "cooking" the wood chips in a mix containing sodium hydroxide and sodium sulfur which removes a major part of the lignin.
- Bleached kraft pulp (BKP)—In addition to UKP treatments, fibers were bleached to remove nearly all the residual lignin after cooking by using oxidizing chemicals such as chlorine dioxide, oxygen, ozone or hydrogen peroxide. The residual lignin content depends on the bleaching sequence used.

Chemical compositions are detailed in Table 1. The determination of the lignin content was carried out according to the Klason method (TAPPI T222 and TAPPI T250 standards). The analysis of the monosaccharides was performed according to the standard TAPPI T249 om-85. The extraction was carried out using a Soxhlet extractor. Water and then acetone were used as solvents.

Paper making

Papers with a low basis weight of 30 g/m^2 were made up of the four different pulps using an automated dynamic handsheet former (FDA, Techpap, Grenoble, France). FDA uses a process that mimics the industrial sheet production process. The sheet was formed by the projection of pulp onto a wire positioned on a rotating cylindrical jar. The wire was completely submerged in a water wall. The pulp was projected using an injector nozzle fixed on a delivery tube sweeping vertically up and down inside the rotating cylindrical jar. A scoop system bailed out the water wall after the sheet was formed, and the water remaining in the sheet was drained by centrifugal

Table 1 Chemical composition of the different softwood pulps used for paper making

Components	TMP	CTMP	UKP	BKP
Cellulose (%)	45.6	48.7	78.1	80.4
Lignins (%)	26.5	25.8	2.5	0.0
Glucomannans (%)	18.2	19.2	9.3	10.9
Xylans (%)	7.2	6.7	9.4	8.4
Extractives (%)	2.5	0.6	0.7	0.3

force. After the sheet was drained, it was removed along with the wire from the cylindrical jar for pressing and drying. Then, the sheet was dried under constrain at 95 °C during 10 min. To study the influence of sheet density on adhesion, some paper handsheets were also pressed before drying either using a roller press or a calender.

To investigate the influence of the moisture content (MC), some papers were sprayed with water and sponged with blotting paper before ultrasonic welding. After verification, this technique for wetting papers turned out to be very reproducible (MC±1%) and led to a total moisture content of 69%, 68%, 65% and 58% for TMP, CTMP, UKP and BKP, respectively.

The influences of the density and the paper surface properties on the performance of the welded joint were also studied. The structure of the paper fibrous network was modified following two strategies: (1) by wet pressing (before drying) at 0.25 MPa to decrease the porosity of the network or (2) by calendering (after drying) at 10 MPa to decrease the porosity and to increase the surface smoothness simultaneously.

Welding

An ultrasonic welder (Omega III DG—MCX, Mecasonic, Juvigny, France) was used to assemble papers. The technique consisted in applying simultaneously a constant average compression stress (3.75 or 5.00 MPa) and a forced 20 kHz vibration of 60 µm amplitude during a given time between 1 s and 4 s. The compression load was maintained after welding during 10 s. In order to compensate for flatness defects, the following assembly was used: the two test pieces, 50 mm in width and 80 mm in length, were sandwiched between two aluminum foils and then placed between two pieces of cardboard. Then, this assembly was carefully placed between the sonotrode and the anvil. The dimension of the zone subjected to ultrasonic compression was 32×4 mm^2 (Fig. 1). These experiments were carried out at 23±2 °C and 45±5% of relative humidity. Welding was performed on 30 g m^{-2} papers made of each pulp both in dry state (6% moisture content) and in wet state (moisture content around 60%) ("Paper making" section).

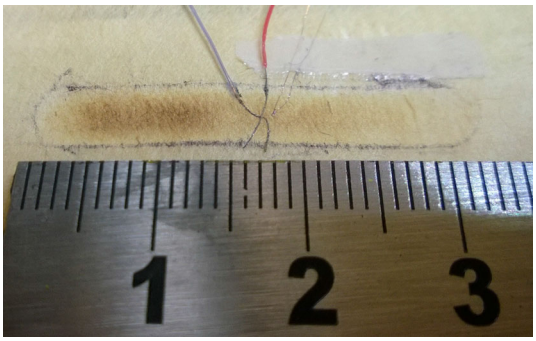

Figure 1 T-type thermocouples for measuring temperature at the interface between two papers during ultrasonic compression.

Gluing

Reference-bonded papers were prepared using hot-melt adhesives. These samples were used as reference to assess the bonding strength of the welded papers with the peeling test presented further. Hot-melt gluing was carried out using a hot-melt glue applicator (Getra, Saint-Amé, France). A glue bead was applied to bond papers on a surface comparable with the welded zone. A commercial hot-melt glue Technomelt Cool 120 (Henkel) adapted to glue papers and boards was used.

Characterization methods

Temperature measurement

In order to explain some phenomena taking place during ultrasonic welding, the temperature of the test pieces during ultrasonic compression was monitored with T-type thermocouples (copper/constantan). Laboratory-made thermocouples were placed between the two pieces of paper to be welded and in the center of the contact area (Fig. 1). An ADC-24 data logger (PicoTechnology, Cambridgeshire, UK) was used to acquire the thermoelectric voltage at the frequency of 10 Hz. For an easier handling, thermocouples manufactured at the laboratory with 76-µm-diameter wires (Omega Engineering, UK) were used. As the thickness of the wires may seem large compared to that of the test pieces, comparative experiments were conducted with unsheathed fine gauge thermocouples (25-µm-diameter wires, response time of 3 ms) from Omega Engineering, UK, to ensure the accuracy of the measurements. No significant differences were found and therefore the largest wires were preferred because 25-µm-diameter copper wires

are very fragile. It should be noted that the presence of the cardboard pieces in the assembly minimizes the disturbance caused by the largest thermocouples.

The conversion from thermoelectric voltage to temperature was obtained from the NIST ITS-90 thermocouple database.

Villegas Fernandez reported that thermocouples could concentrate the ultrasonic energy and therefore provide misleading readings [20]. From this point of view, the recorded values should be considered with caution. However, we did not find clear hot spot traces in the thermocouple region. Moreover, comparative tests were made using irreversible thermosensitive labels (RS Pro ranges 160–199 °C, and 204–260 °C from RS components Ltd, UK, and also Testo range 204–260 °C from Testo, Lenzkirch, Germany) that were placed either between the two test pieces or above the top one. It should be noted that these experiments were performed at a lower pressure because of the maximum temperature detectable with the labels. No significant difference was found whatever the position of the label. Indeed, the temperature gradients in the thickness of our materials subjected to pressure must be very small. In addition, the peak temperature values from the thermocouple readings and the labels were in accordance within 20 °C. It should be noted here that a thermal study of the process is out of the scope of this paper. Therefore, considering the measured temperature range and the repeatability of the results (three replicates) obtained with this setup, we concluded that this method provides relevant qualitative information on the heating process in the case of the welding of papers.

Moisture content measurement

The moisture content of papers was evaluated using a moisture analyzer (HE53, Mettler Toledo, Greifensee, Switzerland). Samples were heated up to 105 °C with a halogen lamp until their mass reached equilibrium. The moisture content (MC) was calculated as follows with m_{wet} and m_{dry} being the masses of the sample before and after heating, respectively:

$$MC = 1 - \frac{m_{dry}}{m_{wet}} \quad (1)$$

Peeling tests

T-Peeling tests were performed with a mechanical testing machine (DY—MTS) equipped with a 10-N sensor at a displacement rate of 300 mm min^{-1} following the recommendations of the standard ASTM D1876. Papers were peeled along the width of the welded joint. The peak force per unit width required to separate the welded joint was reported and expressed in N m^{-1}. Specials jaws adapted to low basis weight papers were used (Fig. 2).

Scanning electron microscope (SEM)

The morphology of samples was analyzed using a FEI Quanta 200 microscope in secondary electron mode operating at 10 kV, after surface coating with an Emitech K550X gold–palladium coating device.

X-ray microtomography

X-ray microtomography imaging experiments were performed at the European Synchrotron Radiation Facility (ESRF, ID19 beamline, Grenoble, France) to obtain 3D images of the microstructure of the center of samples (X-ray energy = 19 keV, CCD detector of 2560 × 2560 pixels, voxel size: 0.324^3 μm^3, scanning time < 2 min). The samples were placed horizontally (beamline in the plane of papers during scanning). Reconstructed scans were processed using ImageJ software (U.S. National Institute of Health, Bethesda, USA) in order to binarize the images (between fibers and pores)

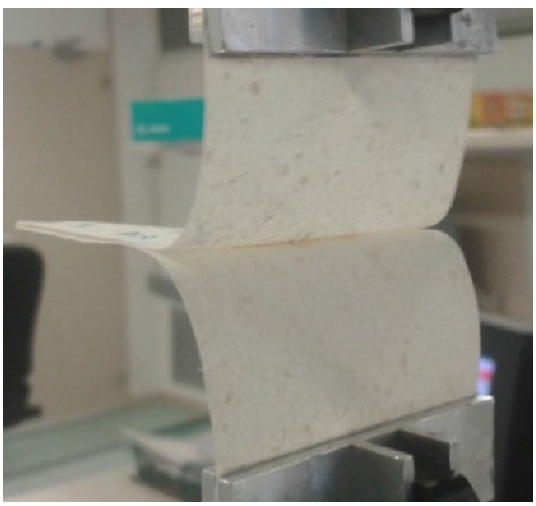

Figure 2 Clamped welded paper strips for T-peel testing of the welded zone (sample width of 50 mm).

and to filter noise [21]. Morphological parameters were evaluated in nine parallelepipedic sub-volumes (base dimensions of 500 × 500 pixels) distributed in the total volume according to Fig. 3. In each sub-volume, the variation of porosity along the thickness of papers was evaluated. For each paper, the averaged variation of porosity was calculated from the nine sub-volumes.

Operative method to optimize the ultrasonic welding process

The four different types of papers were assembled by ultrasonic compression with two compressive stresses of 3.75 and 5 MPa. The temperature at the interface was monitored during ultrasonic compression ("Temperature measurement" section). The optimal temperature necessary to obtain subsequent interfacial bonding without excessively degrading fibers was determined.

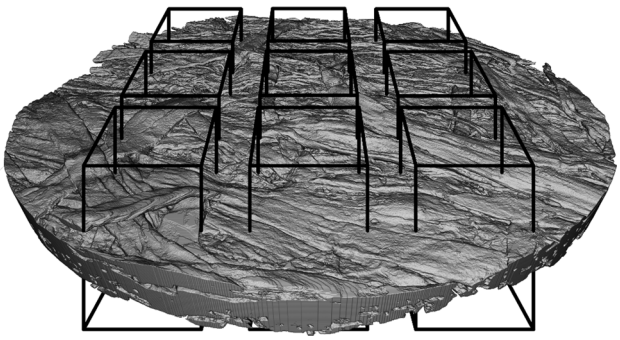

Figure 3 Location of the sub-volumes (black parallelepipeds) used for the determination of papers morphological parameters in 3D X-ray microtomography images (diameter of 830 µm) of welded papers.

This evaluation was based on manual peeling test and on sample observation (color of the bonded zone). Adhesion was judged to be satisfactory when a manual mechanical action is necessary to separate papers, and when delamination occurs in the paper core, paper tears or fibers pullout is observed at the interface. Through trials and errors, it was observed that the best adhesion of the welded joint corresponded to a peak temperature of approximately 350 °C at which a slight coloration of the bonded zone could be observed (Fig. 4). For each dry paper, the approximate ultrasonic compression time necessary to obtain a peak temperature of 350 °C was determined. The repeatability was verified by performing the welding four times with the same conditions. Associated times are reported for each paper in Table 2. They could vary according to the type of paper. At 3.75 MPa, for mechanical pulps, the times varied from 3.0 to 3.5 s depending on the presence or absence of a chemical treatment. For kraft pulps, the times reached up 4.0 s. They were significantly lower at 5 MPa for all paper types. Wet papers were subjected to ultrasonic welding at 5 MPa using the same times than dry papers.

Results

Performance of the paper-to-paper welded joint

Peeling curve profiles and influence of paper nature

The peeling force of the dry papers welded under a compressive stress of 5 MPa is plotted in Fig. 4. Each

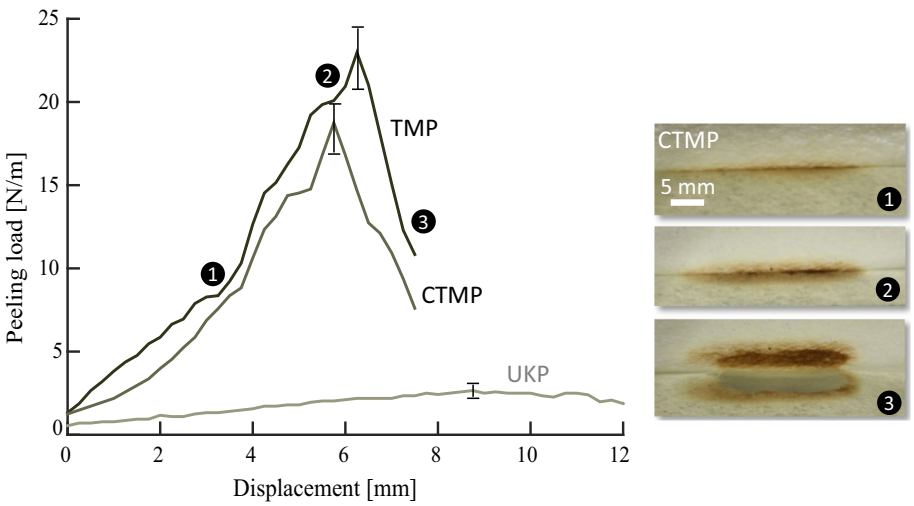

Figure 4 Peeling force per unit width as a function of displacement during peeling tests of dry papers assembled by ultrasonic compression with a compressive stress of 5 MPa.

Table 2 Ultrasonic compression vibration times required to reach a temperature peak of 350 °C at the interface according to the type of pulp and the compressive stresses

Pressure (MPa)	TMP (s)	CTMP (s)	UKP (s)	BKP (s)
3.75	3.00	3.50	4.00	4.00
5.00	1.40	1.50	1.75	1.75

curve represents an average of four different tests. Results clearly show a dependence of the adhesion on the type of paper. The curves of the TMP and CTMP papers depicted the same trend. The force first showed a regular but nonlinear increase (denoted ❶). Both the surrounding area of the bonded zone and the bonded zone were under stress. Because of the geometry of the specimens, it can be roughly assumed that the plies were mostly subjected to bending, whereas the bonded zone was rather subjected to tensile opening stress. The superposition of these two stress states resulted in the nonlinear increase of the peeling force in this first loading stage. As the peeling force reached its maximum value (denoted ❷), the deformation mechanisms in and around the bonded zone became preponderant, resulting in degradation phenomena of papers in the bonded zone and its vicinity. At this stage, it was generally observed that the bonded zone opened. Thus, the maximum peeling force can be considered to be representative of the strength of the bonded zone for an opening failure mode. As illustrated in Fig. 4, this phenomenon also revealed that the bonded zone was colored by the welding process, showing a burnished aspect. Finally in the stage denoted ❸, the force significantly dropped corresponding to the failure of the paper structure around a zone where papers remained bonded. The ultrasonic compression did not induce welding of the BKP papers and the peeling force measured on the welded UKP papers was very low. Peeling tests were also carried out on dry papers welded with a compressive stress of 3.75 MPa. The obtained peeling curves were similar for the TMP and CTMP papers. In addition, the adhesion was negligible for UKP and BKP papers.

Table 3 summarizes the maximal peeling forces per unit width that were recorded for each paper type and each pressure level. The TMP paper exhibited the highest peeling force whatever the applied pressure. The peeling force was 20–30% lower for the CTMP paper, depending on the applied pressure. The peeling forces measured on TMP and CTMP samples assembled by hot-melt gluing are also given in Table 3. For CTMP papers, welded and glued samples performances were in the same range of magnitude, whereas the performance of glued papers was greater for TMP papers. For glued papers, the peak force was recorded when one of the two papers began to fail in its thickness through delamination of the fibrous layers. In paper converting industry, the occurrence of failure during peeling in the thickness of one of the two papers by delamination is considered as a relevant criterion for qualifying well-bonded interfaces. In the case of papers bonded by ultrasonic welding, the failure occurred in the vicinity of the bonded zone: the fiber network was in-plane broken. Thus, the ultrasonic compression could indirectly weaken the fiber network around the effectively bonded zone, by imposing a sudden drying on fibers because of the temperature rise.

Influence of the paper moisture content

Figure 5 shows the curves of the peeling tests conducted on the wet papers assembled by ultrasonic compression at 5 MPa. The curve profiles differed from those obtained for the dry papers. The peeling force reached a plateau-like maximum value whatever the pulp grade, corresponding to the separation of both papers along the 4 mm length of the bonded interface. No paper structure failure occurred. The pictures in Fig. 5 reveal that the bonded zone was not colored but tended to be translucent. For all wet papers, the recorded maximum peeling forces were generally greater compared to those obtained for dry

Table 3 Mean peak load measured during peeling tests of papers assembled by ultrasonic compression or by hot-melt gluing

	TMP (N/m)	CTMP (N/m)	UKP (N/m)	BKP (N/m)
Welding at 3.75 MPa	20.7±2.5	14.6±0.5	0	0
Welding at 5.00 MPa	23.8±1.9	19.2±1.6	3.1±0.4	0
Hot-melt gluing	35.5±5.7	22.1±6.8	–	–
Welding of wet papers (5 MPa)	38.2±4.3	19.8±2.1	8.7±0.9	8.4±0.8

papers (Table 3). For TMP papers, the maximum force reached was 38.2 N m^{-1} for wet papers compared to 23.8 N m^{-1} for dry papers. Thus, for TMP and CTMP papers, the performance became equivalent to that of glued samples. However, as in the previous experiments, the failure modes differed. The ultrasonic compression could contribute to densify the fiber network in the paper thickness, as suggested by the translucent aspect of the welded zone, and consequently prevent from delamination phenomenon. These results also suggest that ultrasonic compression can result in bonded papers which behave as papers bonded using conventional gluing process, provided that the moisture content of the papers has been well adjusted before welding.

Evolution of the temperature at the welded joint

Figure 6 shows the temperature evolution at the interface during ultrasonic compression of dry papers. First, the temperature sharply increased up to 150–200 °C. Then, it continued increasing but with a lower slope until a maximum temperature close to 350 °C. The slope was significantly steeper at 5 MPa, indicating that the increase in heat generation was faster for higher compressive stresses, as it has been reported for the welding of thermoplastics [20]. Besides, the slope was steeper for the TMP paper compared to UKP and BKP papers, which explains why the optimal welding time was lower for the TMP paper (Table 2).

Figure 7 shows the temperature measured with the thermocouple located at the interface of the TMP and BKP wet papers during ultrasonic compression at 5.00 MPa. Compared to dry papers, these curves were similar in the first stage. Then, between 130 and 150 °C, a pronounced curve inflection was observed. Beyond this point, the slope was significantly lower. The maximum temperature reached by wet papers was much lower than those observed in dry papers (around 260–280 °C). It should be noted here that the saturation temperature of water at 5 MPa is 264 °C. Therefore, as long as the papers remain saturated with water, temperature cannot exceed that value. However, the phenomena taking place are complex for several reasons:

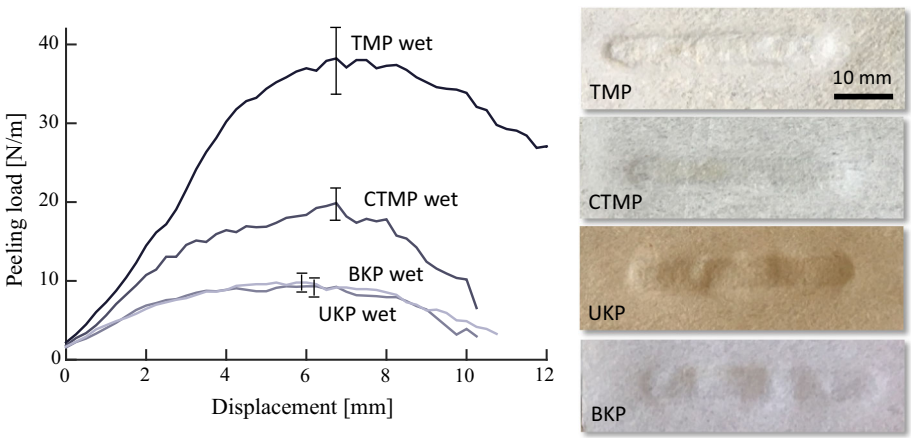

Figure 5 Peeling force per unit width as a function of displacement during peeling tests of wetted papers assembled by ultrasonic compression with a compressive stress of 5 MPa.

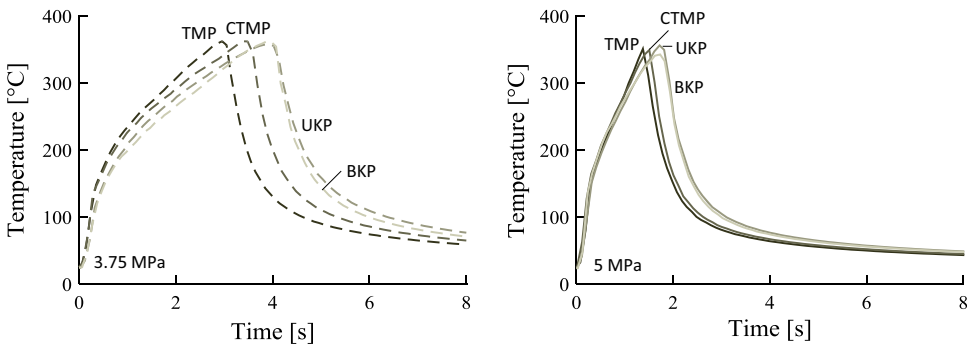

Figure 6 Temperatures recorded during the ultrasonic compression of papers with a compressive stress of 3.75 MPa and 5 MPa.

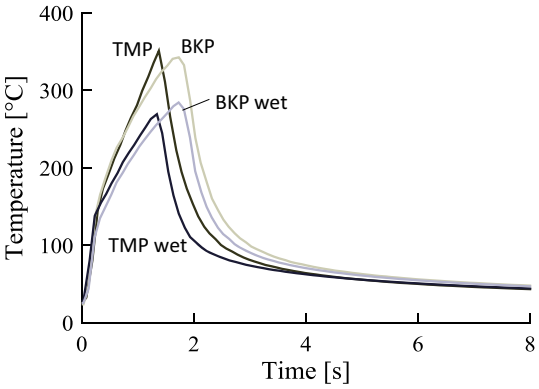

Figure 7 Temperature recorded during the ultrasonic compression of standard and wet papers with a compressive stress of 5 MPa.

- the presence of water may change ultrasound absorption,
- the thermal properties of the medium are higher in the presence of water,
- the amount of water in the medium is unknown because when pressure is applied onto the material some water starts to flow out of the material (wet pressing),
- the temperature promotes water removal because of the decrease in water viscosity and, if water starts to boil, the water vapor will contribute to the removal of water from the material.

Taking into account the accuracy of our measurements, the peak value is in accordance with water starting to boil.

Nonetheless, considering our objectives here, we can only say that since material degradation is most likely to occur in wood fiber polymers beyond 300 °C, these lower temperatures could be at the origin of the translucent-like aspect of the bonded zones in wet papers compared to the burnished aspect of the bonded zones in dry papers.

Structural characterization of the welded joint

Figure 8 shows images obtained using scanning electron microscopy (SEM) of paper surfaces before ultrasonic compression and after peeling for all paper grades. Before welding, the TMP and CTMP papers exhibited both fibers and fine elements from fibers cut or damaged by the mechanical process. The UKP and BKP papers were only made of long and straight fibers clean from any residues, as expected for papers

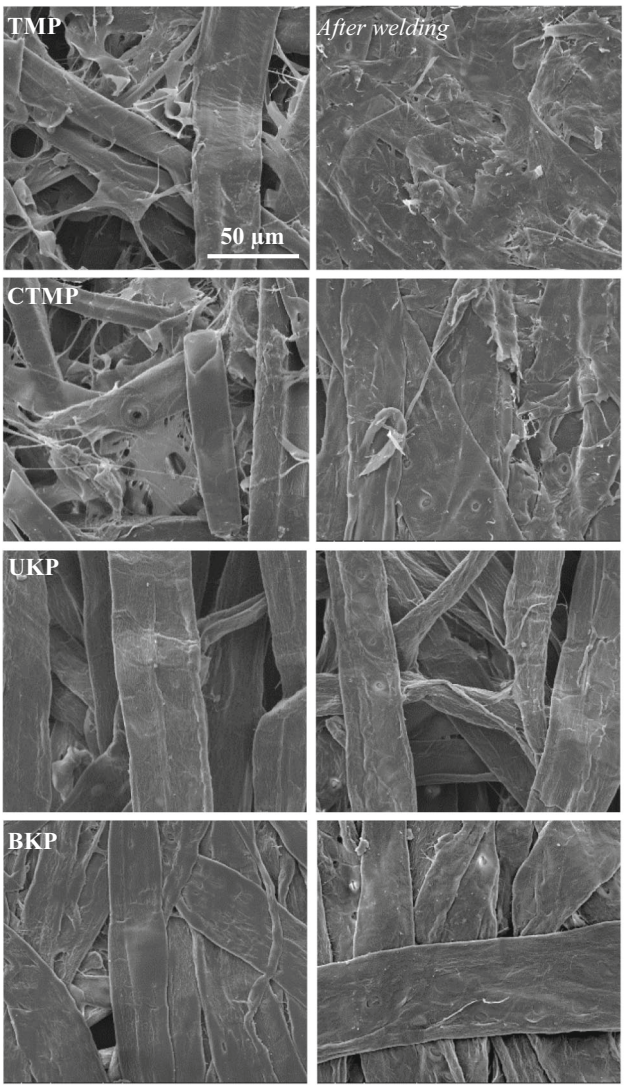

Figure 8 Scanning electron micrographs of unwelded (first row) and welded interface after peeling tests (second row) of TMP, CTMP, UKP and BKP papers, assembled by ultrasonic compression with a compressive stress of 5 MPa.

from pulps obtained by a chemical process. After ultrasonic compression, TMP and CTMP fiber networks seemed dense and rather continuous, while UKP and BKP were mostly sparse fiber networks with significant voids. Finally, the interfaces of TMP and CTMP papers after ultrasonic compression and peeling revealed the presence of fibrils ripped off from the fibers, suggesting that fibers were embedded in a continuous media at the interface. On the contrary, UKP and BKP paper interfaces were undamaged, which corroborates with the measured low peeling forces.

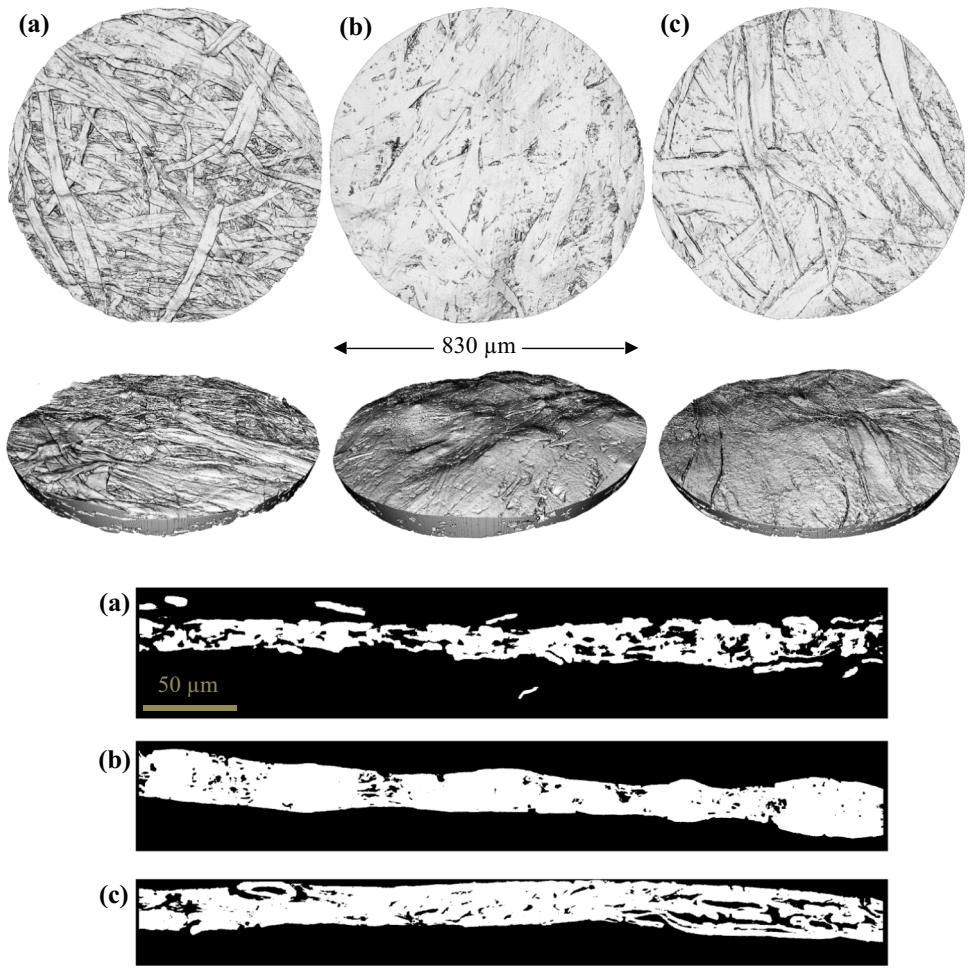

Figure 9 Surface topography and through-thickness cross section obtained by X-ray microtomography of BKP (**a**), TMP (**b**) and wet TMP (**c**) papers welded by ultrasonic compression with a compressive stress of 5 MPa. Note that in cross-section images, fibers are in white and pores/air are in black.

Figure 9 represents the zones subjected to ultrasonic compression of UKP, TMP and wet TMP papers that were imaged by X-ray microtomography. The TMP fiber network appeared to be denser than the UKP fiber network. The TMP paper structure was quasi-continuous: fibers could not be distinguished, which is consistent with SEM observations. Figure 10 depicts the porosity profile in the thickness direction which was evaluated for each sample. As observed, it is no longer possible to distinguish the interface. Indeed densification occurs in all the assembly, at the interface as well as within the paper bulk because of the applied pressure. The dry and wet TMP papers exhibited a homogeneous porosity, while the porosity of the UKP paper varied significantly through the thickness. The minimum average porosity reached 6% for the TMP paper and 20% for the UKP paper. The TMP paper assembled while wet showed a minimum average porosity of 12%. The discrepancy between papers with and without wetting is related to the presence of gaps in the vicinity of fiber edges, as observed in Fig. 9c. The origin of these gaps might be ascribed to the shrinkage of fibers resulting from their drying induced by their heating during ultrasonic compression.

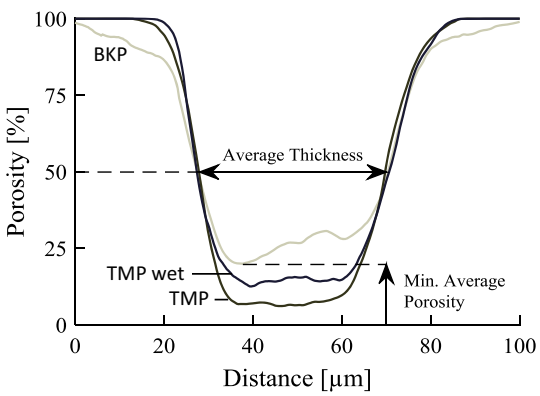

Fig. 10 Porosity distribution along the thickness of papers welded by ultrasonic compression with a compressive stress of 5 MPa.

Table 4 Thicknesses of BKP, TMP and wet TMP papers before and after compression at 5 MPa, and after ultrasonic compression, as well as minimum porosity after ultrasonic compression

Property	BKP	TMP	Wet TMP
Thickness (μm)			
Initial	187.9	304	322
After compression at 5 MPa	43	50	–
After ultrasonic compression at 5 MPa	42.9	41.9	43.2
Minimum average porosity (%)	20.0	6.1	12.5

Table 4 shows the thickness of papers depending on the applied process. Despite significant differences between the thicknesses of unwelded TMP and BKP papers, their thicknesses were very similar after ultrasonic compression. The thicknesses were also measured under 5 MPa without ultrasonic welding to distinguish the contribution of the pressure from the contribution of ultrasonic compression to the densification phenomena. For the BKP paper, the thickness after ultrasonic compression was similar to the thickness measured at 5 MPa, suggesting that ultrasonic welding had no impact on the densification of the fiber network. On the contrary, for the TMP paper, the thickness after welding was 15% lower than the thickness measured at 5 MPa. This result suggests that the material was densified by ultrasonic compression. This result is in accordance with the observation made by SEM showing the formation of a rather continuous material at the interface made of fibers embedded in a wood polymer matrix.

Discussion

Welding papers by ultrasonic compression is effective for TMP and CTMP papers: the level of bonding strength is equivalent to the performance achieved by gluing using hot-melt adhesives. The structural characterization revealed that the welding joint is a quasi-continuous media. TMP and CTMP fibers are composed of 25% lignin and 25% hemicelluloses. These polymers obviously played a key role in the development of bonding strength. In situ measurements revealed that the temperature at the interface exceeded the glass transition temperatures of wood fiber polymers, which is close to 200 °C for lignin and lower for hemicelluloses and amorphous cellulose [8]. This behavior is consistent with the 'thermoplastic' mechanism observed in friction of wood or thermo-compression of natural fiber panels [9, 17], where lignin and, in a lesser extent, hemicelluloses flow from fibers primary wall and middle lamellae to form the matrix of the welded joint. However, for dry papers, the bonded zone was colored. This phenomenon suggests that degradation of wood polymers also took place. Deeper investigations should be carried out to identify the nature of the chemical reactions that occurred, in order to determine if a 'thermosetting' mechanism consecutive to degradation phenomena was also activated. This 'thermosetting' mechanism, which is necessarily preceded by the 'thermoplastic' one, may be of interest to reinforce the matrix by lignin polycondensation reactions or to develop covalent bonding between matrix and fibers provided that degradation phenomena are not too severe.

When the papers were wetted before ultrasonic compression, higher peeling strengths were measured, although the bonded zone was more porous. The glass transition temperature of wood fiber polymers is known to decrease with the water content. For instance, the glass transition temperature of lignin drops to 80 °C at 20% water content [22]. It can be assumed that this plasticizing effect promotes lignin and hemicelluloses flowing and matrix forming after cooling [23]. Besides, a lower temperature (280 °C vs. 350 °C) was reached at the interface for the same welding conditions. As the paper thickness was very small, the water was expected to be fully removed after welding [24]. Thus, it can be fairly assumed that the initial difference in water content between dry and wet papers explains the changes in peak temperature. For wet papers, a larger part of the welding energy was used to vaporize water. This phenomenon could contribute to limit the increase in temperature at the interface and, thus, to decrease the material degradation. However, it is not possible to fully conclude on the role of water to the increase in the bonding strength. Does water act only through limiting the polymer degradation or also help to develop chemical interactions? Finally, this result suggests that adjusting the paper water content may

be a good way to control the heat generation at the interface. Therefore, controlling the water content could be beneficial to an industrial ultrasonic welding process of papers and boards.

Conclusion

This study is an evaluation of the effectiveness of ultrasonic compression for assembling 100% lignocellulosic papers. Several types of papers made of pulp fibers that exhibited various lignin, hemicelluloses and amorphous cellulose contents were tested. Papers of 30 g/m^2 were fabricated using a laboratory dynamic handsheet former. Ultrasonic compression was carried out using an ultrasonic welder dedicated to thermoplastic polymer pieces at a frequency of 20 kHz, for two levels of pressure. For welding, papers were either dry or moistened. For comparison purpose, several papers were assembled using hot-melt adhesives. The interface between bonded papers was characterized using SEM and 3D X-ray microtomography. The temperature was measured with T-type thermocouples placed between the two pieces of paper. This method was considered relevant to provide at least qualitative information.

Results showed that the measured peeling forces were similar to those achieved by hot-melt gluing for papers containing lignin. However, the bonded zone exhibited a burnished aspect. In situ temperature measurements showed that the optimal welded joint performance was obtained for a temperature at the interface around 350 °C. After peeling, the interface showed fibrils ripped off from the fibers suggesting that fibers were embedded in a continuous media at the interface. When papers were wet before ultrasonic compression (moisture content between 58 and 69% depending on the papers), the peeling force increased and the peak temperature dropped to 280 °C. The bonded zone did not turn brown as for dry papers. Instead, they were somewhat translucent. The analysis of SEM micrographs, microtomography images and temperature measurements suggested that the development of adhesion originated from a thermoplastic mechanism. The amorphous polymers of wood (lignin and hemicelluloses) creeped while the temperature was above their glass transition temperatures and formed a matrix that coated fibers and filled the voids in between. This mechanism was assumed to be significantly enhanced in wet papers because of the decrease in the glass transition temperature of polymers in the presence of water. However, the burnished aspect observed on dry papers suggested that degradation of wood polymers also took place. Fully understanding these mechanisms and the actual role of water as well as finely controlling the process are essential in view of broadening the range of papers that can be ultrasonically welded. This would make economically viable this adhesive-free technology for assembling papers and boards.

Acknowledgements

The authors acknowledge the financial support from Institut Carnot PolyNat (ANR-16-CARN-0025-01). P. J.J. Dumont gratefully acknowledges the research site of INSA-Lyon at Oyonnax for administrative support. 3SR and LGP2 are part of the LabEx Tec 21 (Investissements d'Avenir-Grant agreement no. ANR-11-LABX-0030).

References

[1] Confederation European of Paper Industry (2017) Key statistic report. http://www.cepi.org/system/files/public/documents/publications/statistics/2018/210X140_CEPI_Brochure_KeyStatistics2017_WEB.pdf. Accessed 14 June 2019

[2] Lévy A, Le Corre S, Fernandez Villegas I (2014) Modeling of the heating phenomena in ultrasonic welding of thermoplastic composites with flat energy directors. J Mater Proc Technol 214:1361–1371

[3] Volkov SS (2015) Analysis of the process of heat generation in ultrasonic welding of plastics. Weld Int 29:321–324. https://doi.org/10.1080/09507116.2014.921384

[4] Zhang Z, Wang X, Luo Y, Zhang Z, Wang L (2010) Study on heating process of ultrasonic welding for thermoplastics. J Thermoplast Compos 23:647–664

[5] Han W, Liu J, Chong D, Yan J (2015) Analysis on heat generation characteristics in ultrasonic welding of plastics under low amplitude conditions. J Polym Eng 36:413–419. https://doi.org/10.1515/polyeng-2015-0214

[6] Grewell D, Benatar A (2007) Welding of plastics: fundamentals and new developments. Int Polym Proc 22:43–60. https://doi.org/10.3139/217.0051

[7] Pintiaux T, Viet D, Vandenbossche V, Rigal L, Rouilly A (2015) Binderless materials obtained by thermo-compressive processing of lignocellulosic fibres: a comprehensive review. BioResources 10:1915–1963

[8] Zhang D, Zhang A, Xue L (2015) A review of preparation of binderless fiberboards and its self-bonding mechanism. Wood Sci Technol 49:661–679

[9] Gfeller B, Zanetti M, Properzi M, Pizzi A, Pichelin F, Lehmann M, Delmotte L (2003) Wood bonding by vibrational welding. J Adhes Sci Technol 17:1573–1589. https://doi.org/10.1163/156856103769207419

[10] Ganne-Chédeville C, Properzi M, Pizzi A, Leban JM, Pichelin F (2006) Parameters of wood welding: a study with infrared thermography. Holzforschung 60:434–438

[11] Delmotte L, Ganne-Chédeville C, Leban J, Pizzi A, Pichelin F (2008) CP-MAS 13C NMR and FT-IR investigation of the degradation reactions of polymer constituents in wood welding. Polym Degrad Stabil 93:406–412

[12] Omrani P, Pizzi A, Mansouri H, Leban JM, Delmotte L (2009) Physico-chemical causes of the extent of water resistance. J Adhes Sci Technol 23:827–837

[13] Vaziri M, Lindgren O, Pizzi A (2011) Influence of welding parameters on weld line density and its relation to crack formation in welded scots pine joints. J Adhes Sci Technol 25:1819–1828

[14] Sandberg D, Haller P, Navi P (2013) Thermo-hydro and thermo-hydro-mechanical wood processing: an opportunity for future environmentally friendly wood products. Wood Mater Sci Eng 8:64–88

[15] Tondi G, Andrews S, Pizzi A, Leban JM (2007) Comparative potential of alternative wood welding systems, ultrasonic and microfriction stir welding. J Adhes Sci Technol 21:1633–1643

[16] Stamm B (2005) Development of friction welding of wood —physical, mechanical and chemical studies. Ph.D. Dissertation, Ecole Polytechnique Fédérale de Lausanne (Switzerland)

[17] Ganne-Chédeville C (2008) Soudage linéaire du bois: étude et compréhension des modifications physico-chimiques et développement d'une technologie d'assemblage innovante. Ph.D. Dissertation, Université Nancy 1 (France)

[18] Belleville B (2012) Soudage du bois feuillus par friction rotationnelle. Ph.D. Dissertation, Université Laval Québec (Canada)

[19] Navi P, Sandberg D (2011) Thermo-hydro mechanical processing of wood. EPFL Press, Boca Raton. https://doi.org/10.1201/b10143

[20] Villegas Fernandez I (2015) In situ monitoring of ultrasonic welding of thermoplastic composites through power and displacement data. J Thermoplast Compos 28:66–85

[21] Dello S, van Dam R, Slangen J, van de Poll M, Bemelmans M, Greve J, Beets-Tan R (2007) Liver volumetry plug and play: do it yourself with ImageJ. World J Surg 31:2215–2221. https://doi.org/10.1007/s00268-007-9197-x

[22] Salmén L (1984) Viscoelastic properties of in situ lignin under water-saturated conditions. J Mater Sci 19:3090–3096. https://doi.org/10.1007/BF01026988

[23] Bouajila J, Limare A, Joly C, Dole P (2005) Lignin plasticization to improve binderless fiberboard mechanical properties. Polym Eng Sci 45:809–816

[24] Abbasion S, Moonen P, Carmeliet J, Dérome D (2015) A hygrothermo-mechanical model for wood: part B. Parametric studies and application to wood welding. Holzforschung 69:839–849. https://doi.org/10.1515/hf-2014-0190